

# MIMO Channel Model and Correlation Between Channel Matrix Elements in Multipath Channel

Hiroaki NAKABAYASHI, Shota IGARASHI, Tomohiro HAMASHIMA, and Shigeru KOZONO

Members, IEEE

Department of Electrical, Electronics and Computer Engineering, Chiba Institute of Technology

2-17-1 Tsudanuma, Narashino-shi, 275-0016, Japan

E-mail: kozono.shigeru@it-chiba.ac.jp

**Abstract**— To clarify MIMO channel complex correlation for various cell types, we studied the correlation analytically and by computer simulation. We prepared a MIMO channel model consisting of base and mobile antenna configurations and a delay profile with arriving and incident wave angles ( $\xi_m, \zeta_n$ ) in line-of-sight (LOS) and non-line-of-sight (NLOS) paths. Then, the general correlation formula  $\rho_{i,j,i',j'}(bm)$  was derived for the model. It shows that  $\rho_{i,j,i',j'}(bm)$  depends on two factors: antenna configuration at mobile and base sites ( $z_{i-i}, z_{j-j}, \psi_{i-i}, \psi_{j-j}$ ) and angle distribution ( $\xi_c, \Delta\xi_n, \zeta_c, \sigma$ ). It also shows that  $\rho_{i,j,i',j'}(bm)$  is expressed as the addition of a directive wave term  $k \exp(j\Delta\theta_0)$  to the product of mobile site correlation  $\rho_{i-i}(m)$  and base site correlation  $\rho_{j-j}(b)$  without LOS, which are calculated independently of each other. So, the formulas for  $\rho_{i-i}(m)$  and  $\rho_{j-j}(b)$  were derived for uniform and Gaussian angular distributions. Furthermore, a computer simulation was performed and the simulated and theoretical values agreed well. Therefore, we can apply the  $\rho_{i,j,i',j'}(bm)$  to various cell types indoors and outdoors by combining them, so it is possible to calculate the correlation between MIMO channel matrix elements for a given cell and environment.

**Index Terms**—MIMO channel model, MIMO channel correlation, multipath with LOS and NLOS, arriving and incident wave angles, uniform and Gaussian distributions.

## I. INTRODUCTION

To support realtime multimedia communication, future mobile communications will require a high-bit-rate transmission system with high utilization of the frequency spectrum in multipath channels with line-of-sight (LOS) and non-line-of-sight (NLOS) paths [1]. Systems capable of fulfilling this requirement, with features such as multiple-input multiple-output (MIMO) and orthogonal frequency division multiplexing (OFDM) [2], have been studied extensively. MIMO is especially advantageous in high utilization of the frequency spectrum and has therefore been paid attention from this

viewpoint. In MIMO, transmission quality and capacity depend on the channel matrix property, which is evaluated from the correlation between the channel matrix elements, i.e., mutual channels on the path between antenna elements at base and mobile stations. Therefore, the channel matrix correlation must be clarified, and many such studies have been reported [3] [4]. As an analytical model that tries to produce the matrix with a given fixed spatial correlation between MIMO antenna elements, a stochastic MIMO channel model was analyzed on the basis of an independent and identically distributed (i.i.d) random matrix [5]. However, with the analysis method used in the model, it is difficult to interpret the channel situation directly and visualize the physical propagation in MIMO transmission studies. Moreover, MIMO can operate in a wide area such as indoors and outdoors with LOS and NLOS paths. However, there has been little analytical work on such as a situation, especially on channels with multiple paths between the base and mobile station antennas and with a LOS path. Therefore, this paper analytically clarifies MIMO channel correlation on the basis of the propagation mechanism for various cells and environments and presents confirmation of the derived formulas by computer simulation.

## II. THEORY

### A. MIMO channel model

MIMO systems are used in various areas, so the cells are called pico, micro, and macro cells. The MIMO channel model, which consists of a delay profile measured around the origins at both the base station and mobile station and the antenna coordinate systems are shown in Fig. 1. The delay profile has two angles ( $\xi_m, \zeta_n$ ) incident to multipath scattering and to the receiving point, except for path data with an ordinary delay profile. Moreover, each arriving wave expresses a representative wave, which is the peak value in each cluster. Assuming that the movement distance is within a few wavelengths, an example of a delay profile is shown in Fig. 1 with the following conditions.

- i) The number of arriving waves is  $N+1$ , waves are independent of each other, and the  $n$ th-path wave is

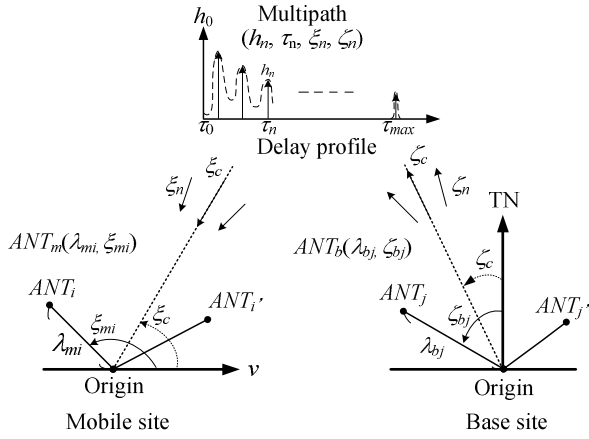


Fig. 1. MIMO channel model.

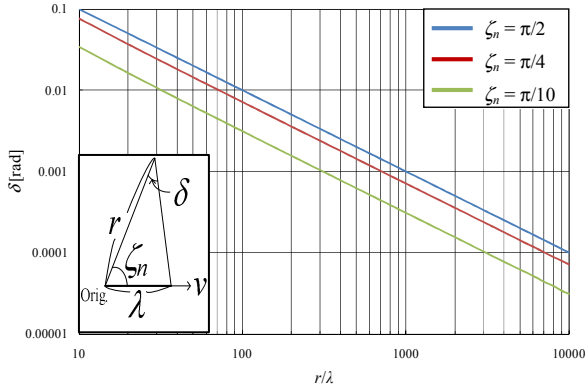


Fig. 2. Angular difference  $\delta$  from  $\xi_n$  or  $\xi_n'$  (for spacing  $\lambda$  from origin).

- denoted by subscript  $n$ , where  $n=0$  means a directive wave and  $n \geq 1$  means no directive waves.
- ii) The waves have excess delay time  $\tau_n$  relative to the shortest path between both origins and maximum excess delay time  $\tau_{max}$ . The  $\tau_n$  values are random from  $\tau_{min}$  to  $\tau_{max}$ .
  - iii) The amplitude is  $h_n$ , the power ratio of the directive and nondirective waves is denoted by  $k$  ( $K$  in dB), and  $k=0$  ( $K=-\infty$  dB) means NLOS. Furthermore, the nondirective wave's power is normalized to 1.
  - iv) Whether a wave's arriving angle at the mobile or base station is also the incident angle to multipath scattering from the mobile or base station depends on whether the station is receiving or transmitting. Here, the angle at the mobile station is denoted by  $\xi_n$  and that at the base station is denoted by  $\xi_n'$ . The  $\xi_n$  and  $\xi_n'$  are angles from the mobile station's movement direction and from true north (TN) at the two origins, respectively. The arriving wave's initial phase is  $\phi_n$  and the values are random from  $-\pi$  to  $\pi$ .

On the other hand, the antenna coordinates use a polar coordinate system centered at the origin of each station, as shown in Fig. 1. For the base station, the coordinates are denoted by  $ANT_b(\lambda_{bj}, \xi_{bj})$ , where  $\lambda_{bj}$  and  $\xi_{bj}$  mean the

radius normalized by wavelength  $\lambda$  and counterclockwise angle from TN for the  $j$ th antenna. For a mobile station, the coordinates are similarly denoted by  $ANT_m(\lambda_{mi}, \xi_{mi})$ . The origins are at mobile and base station antenna elements with  $i=1$  and  $j=1$ , respectively.

In this paper, we assume that all antennas of each station have the same values of  $\xi_n$  and  $\xi_n'$ , but strictly  $\xi_n$  and  $\xi_n'$  differ slightly among antennas by value  $\delta$ . The angular difference  $\delta$  from  $\xi_n$  or  $\xi_n'$  for the normalized distance ( $r/\lambda$ ) between the origin and multipath scattering when the antenna is set at spacing  $\lambda$  away from the origin is shown in Fig. 2. This  $\delta$  is less than 0.01 rad when  $r/\lambda=100$ . As shown later, the correlation is sensitive to  $\xi_n$  or  $\xi_n'$  when the antenna is high and far away and when  $\xi_n$  and  $\xi_n'$  have Gaussian distributions, but not so sensitive to  $\xi_n$  or  $\xi_n'$  when  $r/\lambda$  is small and  $\xi_n$  and  $\xi_n'$  are spread widely, as in the case with mobile stations or indoor cells.

### B. Complex received signal of MIMO channel

Under the conditions described above, the MIMO channel composed of the  $j$ th base station antenna and  $i$ th mobile station antenna is denoted by MIMO  $ch(i-j)$  and the complex received signal level  $E_{i-j}(t, f_c)$  is given by

$$E_{i-j}(t, f_c) = \sum_{n=0}^N h_n e^{j\theta_{i-j,n}} \quad (1)$$

$$\theta_{i-j,n} = 2\pi[f_c \tau_n - f_m t \cos \xi_n - \lambda_{mi} \cos(\xi_n - \xi_{mi}) - \lambda_{bj} \cos(\xi_n - \xi_{bj})] + \phi_n, \quad (2)$$

where  $\theta_{i-j,n}$  is the  $n$ th path phase of MIMO  $ch(i-j)$ ,  $f_c$  is the radio frequency, and  $f_m$  is the maximum Doppler frequency. Furthermore, the third and fourth terms of  $\theta_{i-j,n}$  in brackets depend on the mobile and base station antenna constructions and the phase is different from that at each origin.

### C. Derivation of correlation formula

a) *General formula:* We start by studying the general spatial-cross correlation between MIMO  $ch(i-j)$  and  $ch(i'-j')$ , that is the correlation between MIMO channel matrix elements: the complex correlation is denoted by  $\rho_{i-j,i'-j'}(bm)$ . With variables of  $x$  meaning  $E_{i-j}(t, f_c)$  and those of  $y$  meaning  $E_{i'-j'}(t, f_c)$  obtained by (1),  $\rho_{i-j,i'-j'}(bm)$  is expressed by

$$\rho_{i-j,i'-j'}(bm) = \frac{\langle x^* y \rangle}{[\langle x^* x \rangle \langle y^* y \rangle]^{1/2}}. \quad (3)$$

Here,  $\langle \rangle$  and  $*$  mean ensemble average and conjugate complex, respectively. Assuming that  $N$  is a large number under the delay profile in II-A, we start to calculate the denominator in (3). Each value  $\langle x^* x \rangle$  and  $\langle y^* y \rangle$  is  $k+1$  since the nondirective wave's power is normalized to 1. Therefore, the denominator becomes  $k+1$ . Next, we calculate  $\langle x^* y \rangle$ , i.e.,  $\langle E_{i-j}(t, f_c)^* E_{i'-j'}(t, f_c) \rangle$ , in the numerator. Since  $\tau_n$  and  $\phi_n$  are random values, the  $\theta_{i-j,n}$  given by (2) becomes a random value in the range from  $-\pi$  to  $\pi$ , moreover,  $\theta_{i-j,n}$  is independent of  $h_n$ . As a result, the sum of the product of  $E_{i-j}(t, f_c)^*$  and  $E_{i'-j'}(t, f_c)$  remains

the same for the  $n$ th arriving wave on  $ch(i-j)$  and  $ch(i'-j')$ , but vanishes for all other differences for that, and we get (4), considering that the directive wave is deterministic within a few wavelengths through consideration of the correlation, where  $\Delta\theta_n$  expresses the  $n$ th path phase difference between MIMO  $ch(i'-j')$  and  $ch(i-j)$ .

$$\begin{aligned} \langle x^* y \rangle &= \langle \sum_{n=0}^N h_n^2 \exp(j\Delta\theta_n) \rangle \\ &= \langle h_0^2 \exp(j\Delta\theta_0) \rangle + \langle \sum_{n=1}^N h_n^2 \rangle \\ &\times \langle \sum_{n=1}^N [\cos(2\pi z_{i-i'} \cos(\xi_n - \psi_{i-i'})) - j \sin(2\pi z_{i-i'} \cos(\xi_n - \psi_{i-i'}))] \rangle \\ &\times \langle \sum_{n=1}^N [\cos(2\pi z_{j-j'} \cos(\xi_n - \psi_{j-j'})) - j \sin(2\pi z_{j-j'} \cos(\xi_n - \psi_{j-j'}))] \rangle \quad (4) \\ &= k \exp(j\Delta\theta_0) + \rho_{i-i'}(m) \cdot \rho_{j-j'}(b) \quad (5) \end{aligned}$$

The  $z_{i-i'}$ ,  $\psi_{i-i'}$  and  $z_{j-j'}$ ,  $\psi_{j-j'}$  are antenna construction parameters calculated by (6) for the mobile station.

$$\begin{aligned} z_{i-i'} &= [a^2 + b^2]^{1/2}, \quad \psi_{i-i'} = \tan^{-1}(b/a) \quad (6) \\ a &= \lambda_{mi} \cos \xi_{mi} - \lambda_{mi} \cos \xi_{mi}, \quad b = \lambda_{mi} \sin \xi_{mi} - \lambda_{mi} \sin \xi_{mi} \end{aligned}$$

The first and second terms in (4) are concerned with a directive wave and nondirective waves. Moreover, three ensemble averages in the second term are nondirective power, mobile station, and base station factors, respectively. So we can calculate these averages independently and denote them as in (5). From the above description, we can get  $\rho_{i-j,i'-j'}(bm)$  by rewriting (3) as (7), where  $\rho_{i-i'}(m)$  and  $\rho_{j-j'}(b)$  are mobile and base site correlations without a directive wave, respectively.

$$\rho_{i-j,i'-j'}(bm) = [k \exp(j\Delta\theta_0) + \rho_{i-i'}(m) \cdot \rho_{j-j'}(b)] / (k+1) \quad (7)$$

Though the value of the numerator depends strongly on the first term by a directive wave, it becomes  $\rho_{i-i'}(m)\rho_{j-j'}(b)$  in the case without LOS. Also  $i=i'$  and  $j=j'$  mean  $\rho_{i-i'}(m)=1$  and  $\rho_{j-j'}(b)=1$ , respectively. Furthermore, we expand  $\rho_{i-i'}(m)$  in (7) to a Neumann expansion because the ensemble average is integrated with respect to  $\xi_n$  [6], and we get (8).

$$\begin{aligned} \rho_{i-i'}(m) &= \langle \sum_{n=1}^N [\sum_{l=0}^{\infty} \varepsilon_l (-1)^l J_{2l}(2\pi z_{i-i'}) \cos(2l(\xi_n - \psi_{i-i'}))] \rangle \\ &- j \langle \sum_{n=1}^N [2 \sum_{l=0}^{\infty} (-1)^l J_{2l+1}(2\pi z_{i-i'}) \cos((2l+1)(\xi_n - \psi_{i-i'}))] \rangle \quad (8) \end{aligned}$$

Here,  $\varepsilon_l=1(l=0)$ ,  $\varepsilon_l=2(l \geq 1)$ , and  $J_{2l}(\cdot)$  is a Bessel function of the first order. We can get  $\rho_{j-j'}(b)$  similarly to  $\rho_{i-i'}(m)$ . Finally, we can get the general equation of MIMO channel correlation  $\rho_{i-j,i'-j'}(bm)$  by substituting (8) in (7). From (7),  $\rho_{i-j,i'-j'}(bm)$  is calculated from two items: antenna configuration ( $z_{i-i'}$ ,  $z_{j-j'}$ ,  $\psi_{i-i'}$ ,  $\psi_{j-j'}$ ) and multipath state ( $k$ ,  $\xi_n$ ,  $\zeta_n$ ).

*b) Example of correlation  $\rho_{i-j,i'-j'}(bm)$ :* The  $\rho_{i-j,i'-j'}(bm)$  given by (7) contains the product of  $\rho_{i-i'}(m)$  and  $\rho_{j-j'}(b)$ , which are independent of each other. Therefore, it is sufficient to prepare just one side (either transmitting or receiving) for various environments because we can get  $\rho_{i-j,i'-j'}(bm)$  by combining them. Therefore, we will study the correlation with uniform distribution of  $\xi_n$  and with Gaussian distribution of  $\zeta_n$ .

*i) For uniform distribution of  $\xi_n$ :* We first calculate  $\rho_{i-i'}(m)$  by (8) when  $\xi_n$  for  $n \geq 1$  has a uniform distribution centered at  $\xi_c$  over  $\xi_c - \Delta\xi_n < \xi_n < \xi_c + \Delta\xi_n$  and the probability density function of  $\xi_n$  is  $pdf(\xi_n)=1/2\Delta\xi_n$ . Assuming a large  $N$ , we can calculate the ensemble average in (8) by integration with respect to  $\xi_n$  and we get (9).

$$\begin{aligned} \rho_{i-i'}(m) &= \sum_{l=0}^{\infty} \varepsilon_l (-1)^l J_{2l}(2\pi z_{i-i'}) \frac{1}{2l\Delta\xi_n} \sin(2l\Delta\xi_n) \cos(2l(\xi_c - \psi_{i-i'})) \\ &- j 2 \sum_{l=0}^{\infty} (-1)^l J_{2l+1}(2\pi z_{i-i'}) \frac{1}{(2l+1)\Delta\xi_n} \sin((2l+1)\Delta\xi_n) \cos((2l+1)(\xi_c - \psi_{i-i'})) \quad (9) \end{aligned}$$

*ii) For Gaussian distribution of  $\zeta_n$ :* Next, we calculate  $\rho_{j-j'}(b)$  when  $\zeta_n$  for  $n \geq 1$  has a Gaussian distribution centered at  $\zeta_c$  with deviation  $\sigma$ . Similarly, we get (10).

Table 1. Simulation parameters.

MIMO channel		Base/mobile one-side channel		Base & mobile both-sides channel	
Area		Indoors	Outdoors	Indoors	Outdoors
Incident /arriving angle	Distribution	Uniform	Gaussian	Uni.-uni.	Uni.-Gaussian
	$\xi_c, (\Delta\xi_n)$	0, $(\pi, \pi/2, \pi/4)$	---	0, $(\pi, \pi/2, \pi/4)$	0, $(\pi)$
	$\zeta_c, (\sigma)$	---	$\pi/6, (\pi/90, \pi/36, \pi/18)$	0, $(\pi, \pi/2, \pi/4)$	$\pi/6, (\pi/90, \pi/36, \pi/18)$
Delay profile	$N$	10			
	$h_n$	Exponential distribution			
	$K$	- $\infty$ , 5dB ( $\xi_0=5\pi/6$ )		- $\infty$	
Antenna	$\lambda_m, (\xi_m)$	0 ~ 5, (0)	---	0~5, 0.5, (0)	0~20, 0.5, (0)
	$\lambda_b, (\zeta_b)$	---	0~20, (0)	0~5, (0)	0~20, (0)

$$\rho_{j-j'}(b) = \sum_{l=0}^{\infty} \varepsilon_l (-1)^l J_{2l}(2\pi z_{j-j'}) \cos(2l(\zeta_c - \psi_{j-j'})) \exp(-2l^2 \sigma^2) - j 2 \sum_{l=0}^{\infty} (-1)^l J_{2l+1}(2\pi z_{j-j'}) \cos((2l+1)(\zeta_c - \psi_{j-j'})) \exp(-\frac{(2l+1)^2 \sigma^2}{2}). \quad (10)$$

### III. SIMULATION

#### A. Simulation method

A computer simulation was performed to verify (7), (9), and (10) by using (1), (2), and (3). The simulation parameters are listed in Table 1. As suggesting by (7), we need to simulate two terms: mobile or base site one-sidechannel, i.e.,  $\rho_{i-i'}(m)$  or  $\rho_{j-j'}(b)$  with and without

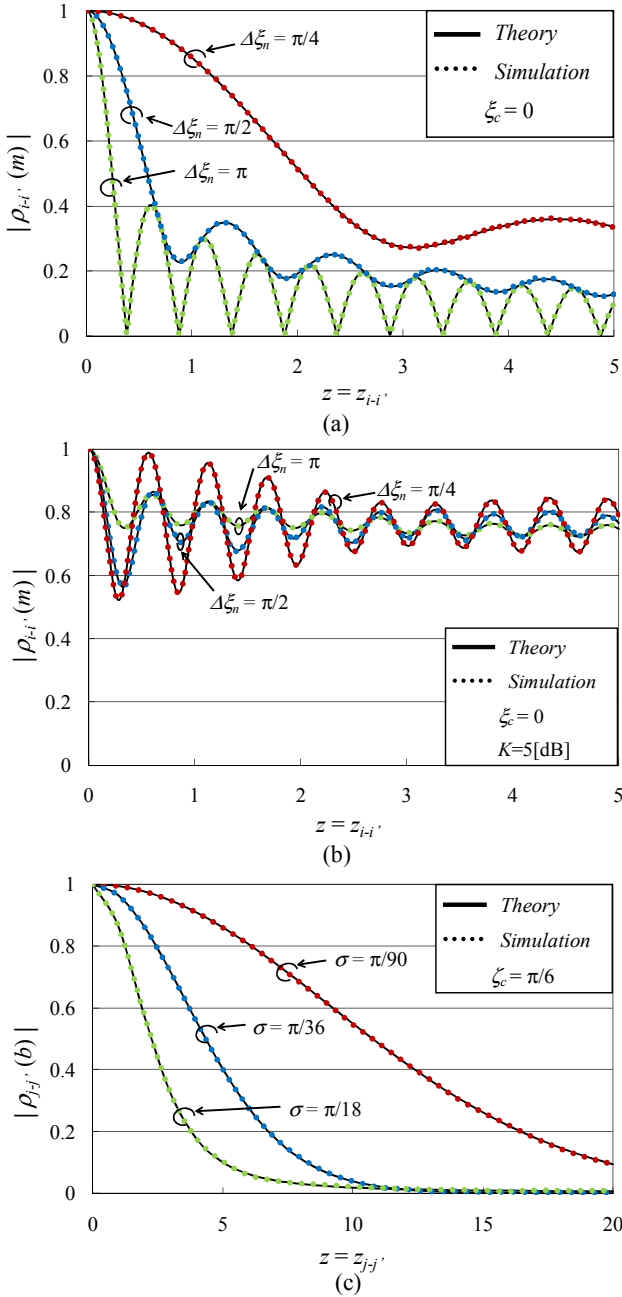


Fig. 3. Correlation of one-side channel. (a) NLOS (uniform distribution). (b) LOS (uniform distribution). (c) NLOS (Gaussian distribution).

the addition of  $k \exp(j\Delta\theta_0)$ , and mobile-base channel, i.e.,  $\rho_{i-j,i'-j'}(bm)$ . The radio frequency  $f_c$  was 3 GHz and the delay profile in II-A was used for uniform and Gaussian distributions. The multipath state  $(k, \xi_n, \zeta_n)$  and antenna parameters  $(\lambda_b, \zeta_b, \lambda_m, \zeta_m)$  were set as shown in Table 1. Each simulated correlation value was calculated from an ensemble average for more than  $10^6$  delay profiles, when the path data such as  $h_n$ ,  $\tau_n$ , and  $\xi_n$  with nondirective waves were changed every delay profile, but a directive wave's data did not change because we assumed a deterministic wave in the set environment. In this way, we performed a statistical analysis.

#### B. Simulation results and discussion

a) Base or mobile site one-side channel: Figures 3(a) and (b) show the absolute value of the correlation simulated for arriving angle  $\xi_n$  with uniform distribution, and Fig. 3(c) shows that with Gaussian distribution, when antenna spacing  $z=z_{i-i'}$ ,  $\psi_{i-i'}=0$ . Figures 3(a) and (b) are for NLOS and LOS with  $K=5$  dB and  $\xi_0=5\pi/6$ , and they also show the theoretical value calculated by (7) with  $j=j'$ ; the simulated and theoretical values agree well. Theory in Fig. 3(a) for  $\Delta\xi_n = \pi$  becomes  $\rho_{i-i'}(m)=J_0(2\pi z_{i-i'})$ , as is well known. The correlation value with Gaussian distribution in Fig. 3(c) is higher than that with uniform distribution.

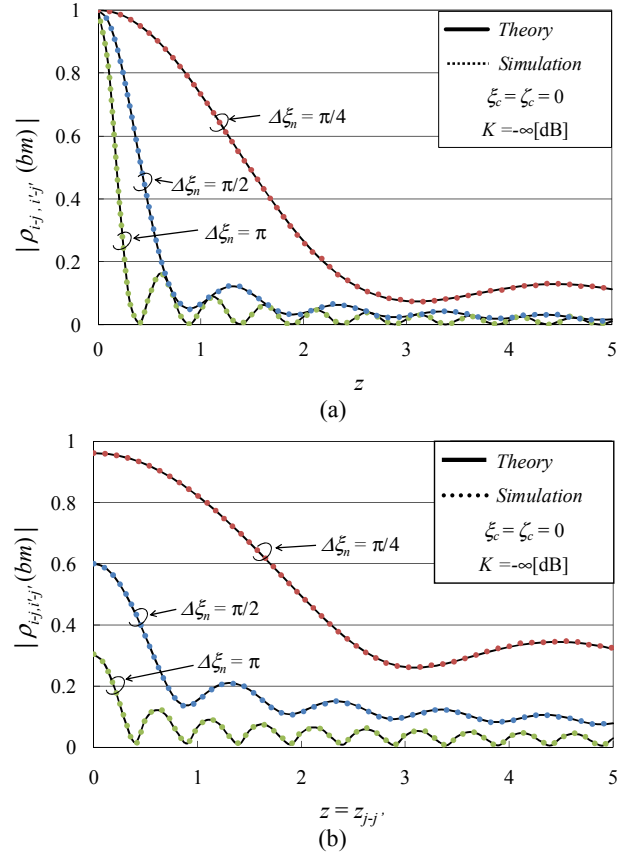


Fig. 4. Correlation between base and mobile channels (uniform-uniform distribution). (a)  $z = z_{i-i'} = z_{j-j'}$ . (b)  $z_{i-i'} = 0.5$ .

The simulated value also agrees with the theory according to (7) with  $i=i'$  and  $k=0$ .

b) *Between base and mobile site channel*: Figure 4 shows the simulated correlation  $|\rho_{i-j,i'-j'}(bm)|$  for both incident  $\xi_n$  and arriving  $\xi_n$  with uniform distribution in NLOS supposing base and mobile sites indoors in the case of different channels between base and mobile sites, i.e.,  $i \neq i'$  at the mobile station and  $j \neq j'$  at the base station. Figure 4(a) shows the simulated correlation when changing  $z=z_{i-i'}=z_{j-j'}$  while keeping  $\psi_{i-i'}=\psi_{j-j'}=0$ . It also shows the theoretical value obtained by (7) with (9), i.e.,  $\rho_{i-j,i'-j'}(bm)$  products of  $\rho_{i-i'}(m)$  and  $\rho_{j-j'}(b)$ , or here  $\rho_{i-j,i'-j'}(bm)=\rho_{i-i'}(m)^2$ . The simulated and theoretical values agree well. Figure 4(b) is the simulated value when changing  $z=z_{j-j'}$  as in Fig. 4(a), except keeping  $z_{i-i'}=0.5$ . The theoretical values of  $\rho_{i-j,i'-j'}(bm)$  were calculated by (7) with (9) as  $\rho_{i-i'}(m)$  for the mobile station is constant at  $z_{i-i'}=0.5$ . The simulated and theoretical values agree well. Figure 5 shows the correlation simulated  $|\rho_{i-j,i'-j'}(bm)|$  for arriving  $\xi_n$  with uniform distribution ( $\xi_c=0$ ,  $\Delta\xi_n=\pi$ ) and incident  $\xi_n$  with Gaussian distribution ( $\xi_c=\pi/6$ ,  $\sigma$  parameter), respectively, supposing mobile and base sites outdoors with NLOS. Figure 5(a) was simulated like Fig. 4(a). The simulated values rapidly become small with increasing  $z$  and  $\sigma$  since they have a site with uniform

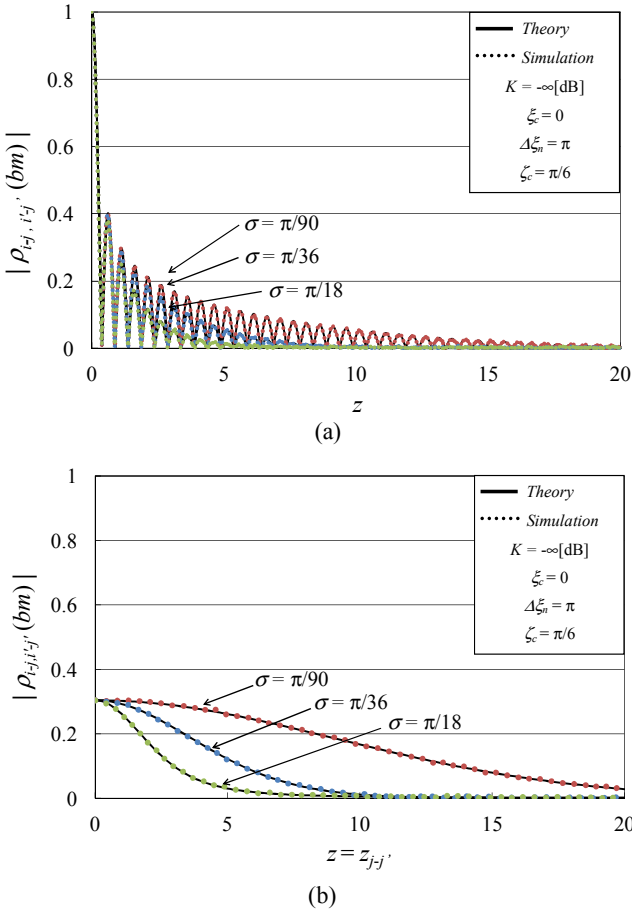


Fig. 5. Correlation between base and mobile channels. (uniform-Gaussian distribution). (a)  $z = z_{i-i'} = z_{j-j'}$ . (b)  $z_{i-i'} = 0.5$ .

distribution. Theoretical value  $\rho_{i-j,i'-j'}(bm)$  obtained by (7) was calculated as  $\rho_{i-i'}(m)$  and  $\rho_{j-j'}(b)$ , corresponding to (9) for the mobile station and (10) for the base station, respectively. The simulated and theoretical values agree well. Figure 5(b) is the correlation simulated by changing  $z=z_{j-j'}$  as in Fig. 5(a), except keeping  $z_{i-i'}=0.5$ . The simulated value is lower than 0.3 whenever  $z$  is small since  $\rho_{i-i'}(m)$  at  $z_{i-i'}=0.5$  is small. The theoretical value was also calculated as in Fig. 4(b). The simulated and theoretical values agree well.

#### IV. CONCLUSION

A MIMO channel model with propagation mechanism was prepared to clarify MIMO channel complex correlation for various cell types and environments. The formula  $\rho_{i-j,i'-j'}(bm)$  between MIMO channel matrix elements was derived and verified by computer simulation. It shows that  $\rho_{i-j,i'-j'}(bm)$  is expressed as the addition of a directive wave term  $k \exp(j\Delta\theta_0)$  to the product of mobile site correlation  $\rho_{i-i'}(m)$  and base site correlation  $\rho_{j-j'}(b)$ , which are calculated independently of each other. The  $\rho_{i-i'}(m)$  and  $\rho_{j-j'}(b)$  were calculated by using two factors: antenna configuration and arriving or incident wave angle distribution. The  $\rho_{i-i'}(m)$  with uniform angle distribution and  $\rho_{j-j'}(b)$  with Gaussian angle distribution were derived. The  $\rho_{i-j,i'-j'}(bm)$  can be applied to various cell types by combining them in indoors and outdoors: therefore, it is possible to calculate the correlation between MIMO channels for a given cell and environment.

#### REFERENCES

- [1] ITU Circular Letter 5/LCCE/2, Radiocommunication Bureau, 7 March 2008.
- [2] T. Hwang, C. Yang, G. Wu, S. Li, and G. Y. Li, "OFDM and Its Wireless Applications: A Survey," *IEEE Trans. Veh. Technol.*, vol. 58, no. 4, pp. 1673-1694, May 2009.
- [3] D. S. Shiu, J. Foschini, M. J. Gans, and M. Kahn, "Fading Correlation and Its Effect on the Capacity of Multielement Antenna Systems," *IEEE Trans. Commun.*, vol. COM-48, no. 3, pp. 502-513, March 2000.
- [4] H. Nishimoto, Y. Ogawa, T. Nishimura, and T. Ohgane, "Measurement-Based Performance Evaluation of MIMO Spatial Multiplexing in Multipath-Rich Indoor Environment," *IEEE Trans. Antennas and Propag.*, vol. 55, no. 12, pp. 3677-3689, Dec. 2007.
- [5] W. Weichselberger, M. Herdin, H. Ozelik, and E. Bonek, "A Stochastic MIMO Channel Model With Joint Correlation of Both Link Ends," *IEEE Trans. Wireless Commun.* vol. 5, no. 1, pp. 90-100, Jan. 2006.
- [6] S. Kozono and S. Sakagami, "Correlation Coefficient on Base Station Diversity for Land Mobile Communication Systems," *IEICE Trans. Commun.*, vol. J70-B, no. 4, pp. 476-482, Apr. 1987.